Measurement of Slow (μs−ms) Time Scale Dynamics in Protein Side Chains by ^{15}N Relaxation Dispersion NMR Spectroscopy: Application to Asn and Gln Residues in a Cavity Mutant of T4 Lysozyme

Frans A. A. Mulder,[†] Nikolai R. Skrynnikov,[†] Bin Hon,[‡] Frederick W. Dahlquist,[‡] and Lewis E. Kay*,[†]

Contribution from the Protein Engineering Network Centres of Excellence and Departments of Medical Genetics, Biochemistry and Chemistry, University of Toronto, Toronto, Ontario, M5S 1A8 Canada, and Institute of Molecular Biology and Department of Chemistry, University of Oregon, Eugene, Oregon, 97403

Received September 20, 2000. Revised Manuscript Received November 9, 2000

Abstract: A new NMR experiment is presented for the measurement of μs−ms time scale dynamics of Asn and Gln side chains in proteins. Exchange contributions to the ^{15}N line widths of side chain residues are determined via a relaxation dispersion experiment in which the effective nitrogen transverse relaxation rate is measured as a function of the number of refocusing pulses in constant-time, variable spacing CPMG intervals. The evolution of magnetization from scalar couplings and dipole−dipole cross-correlations, which has limited studies of exchange in multi-spin systems in the past, does not affect the extraction of accurate exchange parameters from relaxation profiles of NH_2 groups obtained in the present experiment. The utility of the method is demonstrated with an application to a Leu → Ala cavity mutant of T4 lysozyme, L99A. It is shown that many of the side chain amide groups of Asn and Gln residues in the C-terminal domain of the protein are affected by a chemical exchange process which may be important in facilitating the rapid binding of hydrophobic ligands to the cavity.

Introduction

Macromolecular function is dependent on changes in three-dimensional structure in response to specific molecular interactions.[1,2] For example, proteins involved in signal transduction often undergo significant rearrangements in tertiary structure upon ligand binding or covalent modification, such as phosphorylation.[3] In the case of many enzymes, access of ligands to the catalytic site requires transient conformational rearrangements to provide a path of entry.[4] A detailed analysis of molecular dynamics is therefore critical for a complete understanding of function in these systems. Over the past decade NMR spectroscopy has emerged as a powerful technique for studying molecular motion at atomic resolution.[5,6] To date the majority of studies have focused on ps-ns backbone dynamics by measuring ^{15}N spin relaxation properties on a per-residue basis.[7] Recently, methods have also been developed for probing ps−ns motions of side chain atoms in proteins.[8−12] Unlike backbone motions which are largely uniform in most folded proteins, a large variability in the amplitude of side chain dynamics has been observed.[9,10] A number of interesting studies of protein side chain dynamics have provided insight into factors that are important for molecular recognition[13−15] and for protein stability.[16]

While dynamics occurring on fast (ps) time scales largely reflect bond librations associated with small amplitude motions, slower time scale motions may involve more significant excursions that are thought to be necessary for biological function.[17] With this in mind, methodology has been developed for probing backbone motions on μs−ms time scales in proteins.[6] Most experiments involve measuring ^{15}N relaxation rates either as a function of variable spacing in CPMG-based experiments[18−21] or as a function of effective spin-lock field.[22−24]

[†] University of Toronto.
[‡] University of Oregon.

(1) Frauenfelder, H.; Parak, F.; Young, R. D. *Annu. Rev. Biophys. Biophys. Chem.* **1988**, *17*, 451−479.
(2) Karplus, M.; McCammon, J. A. *Annu. Rev. Biochem.* **1983**, *53*, 263−300.
(3) Pawson, T. *Nature* **1995**, 573−580.
(4) Fersht, A. *Enzyme Structure and Mechanism*, 2nd ed.; Freeman & Co.: New York, 1985.
(5) Kay, L. E. *Nat. Struct. Biol. NMR Suppl.* **1998**, *5*, 513−516.
(6) Palmer, A. G. *Curr. Opin. Struct. Biol.* **1997**, *7*, 732−737.
(7) Palmer, A. G.; Williams, J.; McDermott, A. *J. Phys. Chem.* **1996**, *100*, 13293−13310.
(8) LeMaster, D. M.; Kushlan, D. M. *J. Am. Chem. Soc.* **1996**, *118*, 9255−9264.
(9) Muhandiram, D. R.; Yamazaki, T.; Sykes, B. D.; Kay, L. E. *J. Am. Chem. Soc.* **1995**, *117*, 11536−11544.
(10) Wand, A. J.; Urbauer, J. L.; McEvoy, R. P.; Bieber, R. J. *Biochemistry* **1996**, *35*, 6116−6125.
(11) Yang, D.; Mittermaier, A.; Mok, Y. K.; Kay, L. E. *J. Mol. Biol.* **1998**, *276*, 939−954.
(12) Boyd, J. *J. Magn. Res., Ser. B* **1995**, *107*, 279−285.
(13) Kay, L. E.; Muhandiram, D. R.; Farrow, N. A.; Aubin, Y.; Forman-Kay, J. D. *Biochemistry* **1996**, *35*, 361−368.
(14) Kay, L. E.; Muhandiram, D. R.; Wolf, G.; Shoelson, S. E.; Forman-Kay, J. D. *Nat. Struct. Biol.* **1998**, *5*, 156−163.
(15) Lee, A. L.; Kinnear, S. A.; Wand, A. J. *Nat. Struct. Biol.* **2000**, *7*, 72−77.
(16) Desjarlais, J. R.; Handel, T. M. *J. Mol. Biol.* **1999**, *290*, 305−318.
(17) Tolman, J. R.; Flanagan, J. M.; Kennedy, M. A.; Prestegard, J. H. *Nat. Struct. Biol.* **1997**, *4*, 292−297.
(18) Millet, O.; Loria, J. P.; Kroenke, C. D.; Pons, M.; Palmer, A. G. *J. Am. Chem. Soc.* **2000**, *122*, 2867−2877.

10.1021/ja003447g CCC: $20.00
Published on Web 01/16/2001

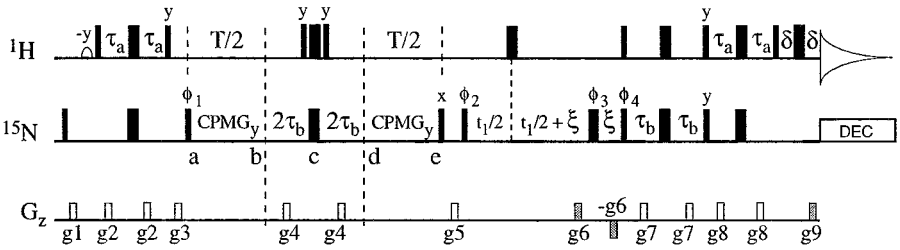

Figure 1. Pulse scheme used to measure relaxation dispersion profiles of NH_2 groups in ^{15}N-labeled proteins. All narrow (wide) pulses are applied with a flip angle of 90° (180°) along the *x*-axis, unless indicated otherwise. The shaped ^1H pulse at the beginning of the sequence is a 7 ms water selective pulse with the EBURP-1 profile.[65] All rectangular ^1H pulses are applied with a field of 35 kHz and are centered at 4.77 ppm. The ^{15}N pulses extending from the 90° pulse of phase $\phi 1$ through to the pulse immediately after point *e* are at a field of 5.0 kHz, while the remaining pulses are applied at 6.5 kHz (all centered at 112 ppm). ^{15}N decoupling is achieved using a WALTZ-16 field[66] (1 kHz at 500 MHz, 1.5 kHz at 800 MHz). Each CPMG*y* element is of the form $(\tau_{CPMG}-180°-\tau_{CPMG})_{n/2}$, where $T = n \times (2\tau_{CPMG} + pw_{N180})$, $n/2$ is even, and pw_{N180} is the ^{15}N 180° pulse width. Quadrature detection in F_1 is achieved using the enhanced sensitivity approach[51,67] where for each value of t_1 separate data sets are recorded for ($\phi 4$,g9) and ($\phi 4+180°$,−g9). The delays used are as follows: $\tau_a = 2.25$ ms; $\tau_b = 1/(8J) = 1.394$ ms, $\zeta = 1.4$ ms, $\delta = 0.5$ ms, $T = 40$ ms. The phase cycle is: $\phi 1 = (x,-x)$; $\phi 2 = 2(x),2(-x)$; $\phi 3 = 2(x),2(-x)$; $\phi 4 = x$; rec = $x,2(-x),x$. For each successive t_1 point $\phi 2$ is incremented by 180° in concert with the receiver.[68] The durations and strengths of the gradients are: $g1$ = (1.0 ms, 5 G/cm); $g2$ = (0.5 ms, 4 G/cm); $g3$ = (1.0 ms, 10 G/cm); $g4$ = (0.5 ms, 18 G/cm); $g5$ = (0.8 ms, −15 G/cm); $g6$ = (1.1 ms, 15 G/cm); $g7$ = (0.4 ms, 3.5 G/cm); $g8$ = (0.3ms, 2.5 G/cm); $g9$ = (0.11 ms, 29.4 G/cm).

Interesting applications of these techniques to protein folding, ligand binding, protein design, motions in proteins and in enzyme catalysis have recently been published.[25−28] Extending these methods to the study of slow dynamic processes involving side chains is of considerable interest. As a first step in this direction we describe herein a CPMG-based relaxation dispersion experiment for measuring exchange at side chain NH_2 positions of Asn and Gln residues in proteins. We show that the effects of scalar coupling and dipole−dipole cross-correlated spin relaxation, which have hampered the extension of methodology to side chain positions in the past,[29] do not limit the measurement of accurate exchange rates.

The utility of the approach is illustrated with an application to a buried cavity mutant of T4 lysozyme, L99A, in which an alanine residue is substituted for a leucine at position 99 in the C-terminal domain of the protein.[30,31] L99A has emerged as a model system for understanding the role of protein dynamics in ligand binding, since the cavity formed by the mutation binds ligands such as substituted benzenes[32] and xenon. Ligand binding occurs rapidly with off-rates of 800 and 300 s^{-1} for benzene and indole at 20 °C, respectively. X-ray structures show that access of ligands is not possible in static structures.[30] The present study establishes that many of the Asn and Gln residues in the C-terminal cavity-containing domain are affected by chemical exchange processes with rates between 350 and 850 s^{-1} and that these slow dynamic modes disappear in the wild-type protein.

Materials and Methods

Sample Conditions and NMR Measurements. A ^{15}N sample of T4 lysozyme (T4L) containing the following mutations, C54T/C97A/L99A, was prepared as described previously.[33] The sample was comprised of 1 mM protein, 50 mM sodium phosphate, 25 mM sodium chloride, pH 5.5. All spectra were collected at 25 °C on Varian Inova 500 and 800 MHz spectrometers. Assignment of side chain NH_2 groups was obtained primarily from analysis of HNCACB[34] and (H)CC(CO)-NH-TOCSY[35,36] spectra.

Relaxation dispersion spectra were recorded as a series of 12 2D data sets with B_1 field strengths, υ_{CPMG}, of 50, 100, 150, 200, 300, 400, 500, 600, 700, 800, 900, and 1000 Hz with repeat experiments recorded at fields of 200 and 500 Hz. In addition, a reference spectrum was obtained by omitting the CPMG intervals in the scheme of Figure 1. Each 2D spectrum was recorded as a complex data matrix comprised of 96 × 512 points or 128 × 768 points at 500 and 800 MHz, respectively. Typically 8 scans/FID were recorded, with a relaxation delay of 2.5 s, resulting in measuring times of 1.1 (500 MHz) and 1.4 (800 MHz) h per spectrum.

The intensities of correlations in each of the experiments were divided by the corresponding intensities of peaks in the reference spectrum, and each relaxation dispersion profile subsequently was fitted using the general equation for two-site exchange[37,38] (see eq 3 of Millet et al.[18]). Errors in extracted parameters were estimated by comparing values obtained from fits of profiles derived from each of the two correlations for a given NH_2 group.

Simulations of Spin Dynamics. The effective relaxation rate, R_2^{eff}, measured using the scheme of Figure 1 is independent of pulse spacing in the absence of exchange. This has been verified by calculating R_2^{eff} for the Asn $^{15}N^{\delta 2}$ and Gln $^{15}N^{\epsilon 2}$ spins of T4 lysozyme as a function of the total number of 180° pulses applied during the constant-time CPMG periods in the sequence, $n(180°)$. The calculations consider the evolution

(19) Loria, J. P.; Rance, M.; Palmer, A. G. *J. Am. Chem. Soc.* **1998**, *121*, 2331−2332.
(20) Ishima, R.; Louis, J. M.; Torchia, D. A. *J. Am. Chem. Soc.* **1999**, *121*, 11589−11590.
(21) Orekhov, V. Y.; Pervushin, K. V.; Arseniev, A. S. *Eur. J. Biochem.* **1994**, *219*, 887−896.
(22) Akke, M.; Palmer, A. G. *J. Am. Chem. Soc.* **1996**, *118*, 911−912.
(23) Mulder, F. A. A.; van Tilborg, P. J. A.; Kaptein, R.; Boelens, R. *J. Biomol. NMR* **1999**, *13*, 275−288.
(24) Zinn-Justin, S.; Berthault, P.; Guenneugues, M.; Desvaux, H. *J. Biomol. NMR* **1997**, *10*, 363−372.
(25) Vugmeyster, L.; Kroenke, C. D.; Picart, F.; Palmer, A. G.; Raleigh, D. P. *J. Am. Chem. Soc.* **2000**, *122*, 5387−5388.
(26) Evenas, J.; Forsen, S.; Malmendal, A.; Akke, M. *J. Mol. Biol.* **1999**, *289*, 603−617.
(27) Ishima, R.; Freedberg, D. I.; Wang, Y. X.; Louis, J. M.; Torchia, D. A. *Struct. Folding Des.* **1999**, *7*, 1047−1055.
(28) Akke, M.; Liu, J.; Cavanagh, J.; Erickson, H. P.; Palmer, A. G. *Nat. Struct. Biol.* **1998**, *5*, 55−59.
(29) Kay, L. E.; Bull, T. E.; Nicholson, L. K.; Griesinger, C.; Schwalbe, H.; Bax, A.; Torchia, D. A. *J. Magn. Reson.* **1992**, *100*, 538−558.
(30) Eriksson, A. E.; Baase, W. A.; Zhang, X. J.; Heinz, D. W.; Blaber, M.; Baldwin, E. P.; Matthews, B. W. *Science* **1992**, *255*, 178−183.
(31) Eriksson, A. E.; Baase, W. A.; Wozniak, J. A.; Matthews, B. W. *Nature* **1992**, *355*, 371−373.
(32) Feher, V. A.; Baldwin, E. P.; Dahlquist, F. W. *Nat. Struct. Biol.* **1996**, *3*, 516−521.
(33) Matsumura, M.; Becktel, W. J.; Matthews, B. W. *Nature* **1988**, *334*, 406−410.
(34) Wittekind, M.; Mueller, L. *J. Magn. Reson., Ser. B* **1993**, *101*, 201−205.
(35) Logan, T. M.; Olejniczak, E. T.; Xu, R. X.; Fesik, S. W. *J. Biomol. NMR* **1993**, *3*, 225−231.
(36) Grzesiek, S.; Anglister, J.; Bax, A. *J. Magn. Reson., Ser. B* **1993**, *101*, 114−119.
(37) Bloom, M.; Reeves, L. W.; Wells, E. J. *J. Chem. Phys.* **1965**, *42*, 1615−1624.
(38) Carver, J. P.; Richards, R. E. *J. Magn. Reson.* **1972**, *6*, 89−105.

of the spin density matrix restricted to the set of four coherences from spins within the NH_2 group, $\{N_+, 2N_+H_{Z,1}, 2N_+H_{Z,2}, 4N_+H_{Z,1}H_{Z,2}\}$, during the period extending from a to e in the scheme of Figure 1 under the effect of spin relaxation, radio frequency pulses, and scalar couplings. The relaxation matrices have been calculated in analytical form using a program written with the Maple symbolic computation software (Waterloo Inc). The elements of the relaxation matrices were subsequently evaluated for 5 Gln and 11 Asn residues in T4 lysozyme using the appropriate set of X-ray coordinates (Protein Database accession code 6LZM;[30] protons were added to the structure which was subsequently refined using the program CNS[39]). Asn163 was omitted from the calculations since there is no density for this residue in the X-ray structure. It has been shown that the order parameters, S^2, describing the amplitudes of motion of the $^{15}N^{\delta 2}-^1H$ and $^{15}N^{\epsilon 2}-^1H$ vectors in hen egg white lysozyme correlate well with the solvent-accessible surface areas of Asn and Gln residues in the protein[40] (correlation coefficient 0.92). We have used this dependence reported by Buck et al.[40] together with the solvent accessible surface areas of individual residues in T4 lysozyme computed using the program Molmol[41] to estimate S^2 for each Asn/Gln residue. Calculated S^2 values vary over a wide range, from 0.2 to 0.9, in agreement with previous experimental observations on related proteins.[40,42] Although order parameters for $^{15}N^{\delta 2}-^1H^{\delta 21}$ and $^{15}N^{\epsilon 2}-^1H^{\epsilon 21}$ dipolar interactions are, in general, lower than for the corresponding interactions involving $^{15}N^{\delta 2}-^1H^{\delta 22}$ and $^{15}N^{\epsilon 2}-^1H^{\epsilon 22}$ dipolar pairs[43] a single order parameter has, nevertheless, been assigned to all spin−spin interactions involving a given NH_2 group. ^{15}N spin relaxation experiments have established that L99A is best modeled as a prolate ellipsoid with a ratio of $D_\parallel/D_\perp = 1.32$, where $D_\parallel = D_{ZZ}$ and $D_\perp = D_{XX} = D_{YY}$ of the axially symmetric diffusion tensor.[44] However, for simplicity, in the present set of calculations we have assumed an isotropic tumbling model with a rotational correlation time of 10.8 ns (25 °C).[44] A value of $T = 40$ ms has been used. All dipolar interactions within the three-spin NH_2 system were included in calculations of the Redfield matrix, as well as the chemical shift anisotropy (CSA) interaction of the ^{15}N spin.[45,46] Both auto- and cross-correlations were considered. In addition, dipolar relaxation resulting from all protons within a radius of 6 Å from the amide nitrogen was included by adding contributions to the auto-relaxation rates of the four coherences of interest.[47] The validity of this approach has been verified by performing complete relaxation calculations including all of the NH_2 spins and the pair of protons closest to the ^{15}N spin (16×16 relaxation matrixes). Although values of R_2^{eff} are altered slightly compared to those obtained with the random field approach, the dependence on $n(180°)$ remains virtually unchanged. It is also possible to include in the simulations contributions from rotation about the $C^\gamma-N^\delta$ (Asn) and $C^\delta-N^\epsilon$ (Gln) bonds that interchange the two amide protons[48] (rate of interconversion on the order of several per second[49]). While this process does not lead to modulation of the ^{15}N chemical shift it nevertheless does affect the evolution of the NH_2 spin system. Simulations (not shown) establish that this interconversion has no effect on extraction of accurate ^{15}N exchange parameters, as expected since exchange of protons in this manner does not directly affect the coherence of interest, $2N_YH_Z$ (see below). Finally, dispersion curves which include the effects of two-site exchange have been simulated by considering spin evolution in the basis $\{N_+^a, 2N_+^a H_{Z,1}^a, ..., N_+^b, 2N_+^b H_{Z,1}^b, ...\}$ where *a* and *b* label the two inequivalent sites with ^{15}N resonance frequencies of ω_N^a and ω_N^b, respectively. The corresponding Zeeman and exchange terms have been included as described by Kaplan and Fraenkel.[50]

Theory

General Considerations. Figure 1 shows the pulse scheme that is used to measure chemical exchange processes involving $^{15}NH_2$ groups in ^{15}N-labeled proteins. The experiment is essentially an enhanced sensitivity HSQC,[51] optimized for application to NH_2 spin systems.[52] At point *a* the coherence of interest is given by $2N_YH_Z$, where N_Y and H_Z are *Y*- and *Z*-components of nitrogen and proton spin operators, respectively, and $H_Z = H_{Z,1} + H_{Z,2}$, with the subscripts 1 and 2 denoting the two attached proton spins. During the interval extending from *a* to *e* in the sequence a fixed number of ^{15}N refocusing pulses are applied during each of the two *constant-time* CPMG intervals of equal length (*a* to *b* and *d* to *e*). A series of 2D spectra are recorded as a function of effective rf field strength by varying the number of 180° pulses and therefore the pulse spacing so that the net relaxation time ($a - b$, $d - e$) is the same in each experiment. The intensities of cross-peaks in 2D spectra recorded for a given rf field, υ_{CPMG}, are converted into decay rates, R_2^{eff}, via

$$R_2^{\text{eff}}(\upsilon_{\text{CPMG}}) = \frac{-1}{T} \ln \frac{I(\upsilon_{\text{CPMG}})}{I_o} \qquad (1)$$

where $I(\upsilon_{\text{CPMG}})$ and I_o are the intensities of a given cross-peak with and without the CPMG periods from *a* to *b* and *d* to *e* in Figure 1, $T/2$ is the length of each CPMG train and $\upsilon_{\text{CPMG}} = 1/(4\tau_{\text{CPMG}})$, with $2\tau_{\text{CPMG}}$ the separation between the centers of successive refocusing pulses. A plot of R_2^{eff} as a function of field strength, υ_{CPMG}, gives a relaxation dispersion profile for each residue from which exchange parameters can be obtained.[18,23]

It is worth emphasizing that in previous methods for measuring relaxation dispersion profiles each point of the dispersion curve is obtained by recording a set of 2D spectra where the length of the CPMG pulse train is incremented with each successive experiment.[19,23,53] Typically 50 or 60 data sets are recorded per profile, resulting in long net measuring times. In contrast, in the present approach only a single spectrum is acquired for each rf field strength since a constant-time scheme is used for *all* of the rf fields employed. Therefore, it is possible to obtain a more complete sampling of the dispersion profile per unit measuring time than with other methods, although each point on the dispersion curve has increased random error. A second and major advantage of using a constant-time CPMG interval is that the evolution of the magnetization of interest

(39) Brünger, A. T.; Adams, P. D.; Clore, G. M.; DeLano, W. L.; Gros, P.; Grosse-Kunstleve, R. W.; Jiang, J.; Kuszewski, J.; Nilges, M.; Pannu, N. S.; Read, R. J.; Rice, L. M.; Simonson, T.; Warren, G. L. *Acta Crystallogr.* **1998**, *D54*, 905−921.
(40) Buck, M.; Boyd, J.; Redfield, C.; MacKenzie, D. A.; Jeenes, D. J.; Archer, D. B.; Dobson, C. M. *Biochemistry* **1995**, *34*, 4041−4055.
(41) Koradi, R.; Billeter, M.; Wüthrich, K. *J. Mol. Graphics* **1996**, *14*, 51−55.
(42) Smith, L. J.; Mark, A. E.; Dobson, C. M.; van Gunsteren, W. F. *Biochemistry* **1995**, *34*, 10918−10931.
(43) Pervushin, K.; Wider, G.; Wuthrich, K. *J. Am. Chem. Soc.* **1997**, *119*, 3842−3843.
(44) Mulder, F. A. A.; Hon, B.; Muhandiram, D. R.; Dahlquist, F. W.; Kay, L. E. *Biochemistry* **2000**, *39*, 12614−12622.
(45) Herzfeld, J.; Roberts, J. E.; Griffin, R. G. *J. Chem. Phys.* **1987**, *86*, 597−602.
(46) Scheurer, C.; Skrynnikov, N. R.; Lienin, S. F.; Straus, S. K.; Bruschweiler, R.; Ernst, R. R. *J. Am. Chem. Soc.* **1999**, *121*, 4242−4251.
(47) Skrynnikov, N. R.; Khazanovich, T. N.; Sanctuary, B. C. *Mol. Phys.* **1997**, *91*, 977−992.
(48) Perrin, C. L. *Acc. Chem. Res.* **1989**, *22*, 268−275.
(49) Guenneugues, M.; Drevet, P.; Pinkasfeld, S.; Gilquin, B.; Menez, A.; Zinn-Justin, S. *Biochemistry* **1997**, *36*, 16097−16108.
(50) Kaplan, J. I.; Fraenkel, G. *J. Am. Chem. Soc.* **1972**, *94*, 2907−2912.
(51) Kay, L. E.; Keifer, P.; Saarinen, T. *J. Am. Chem. Soc.* **1992**, *114*, 10663−10665.
(52) Schleucher, J.; Schwendinger, M.; Sattler, M.; Schmidt, P.; Schedletzky, O.; Glaser, S. J.; Sorensen, O. W.; Griesinger, C. *J Biomol. NMR* **1994**, *4*, 301−306.
(53) Loria, J. P.; Rance, M.; Palmer, A. G. *J. Biomol. NMR* **1999**, *15*, 151−155.

from effects not related to chemical exchange is not important so long as these effects are independent of the pulse spacing in the CPMG trains. For example, in the case of AX_n ($n > 1$) spin systems cross-correlation effects between pairs of AX dipoles renders the relaxation decay nonexponential which complicates analysis in the case where experiments with variable-length CPMG periods are employed, as discussed further below.

A number of features complicate the measurement of μs−ms time scale relaxation properties of ^{15}N or ^{13}C spins in NH_2 and CH_2 spin systems, respectively. First, evolution from the large one-bond X−H scalar coupling interchanges in-phase and anti-phase magnetization components that relax with different rates. Since the rate of application of refocusing pulses during the CPMG train affects the efficiency of in-phase/anti-phase magnetization interchange, a relaxation dispersion profile can be obtained which reflects the difference in relaxation rates of in-phase and anti-phase signals. This compromises extraction of accurate exchange parameters. Recently Palmer and co-workers have developed an elegant method for eliminating this effect in AX spin systems,[19] however, to date, methodology has not been described for application to three-spin AX_2 systems such as side chain amide or methylene groups. A second complicating feature in measuring relaxation properties of ^{15}N or ^{13}C spins with more than a single attached proton is the cross-correlation between pairs of proton-heteronuclear dipolar interactions.[29,54,55] Unlike relaxation interference between CSA and dipolar interactions which can largely be suppressed,[56,57] dipole−dipole cross-correlation effects cannot be easily eliminated and can potentially compromise the extraction of accurate relaxation parameters unless special care is taken. At first glance, therefore, a labeling strategy in which one of the two protons is replaced by a deuteron appears attractive. However, the substantial scalar coupling between the deuteron and the heteroatom of interest (approximately 15 and 20 Hz for ^{15}N−^{2}H and ^{13}C−^{2}H spin pairs, respectively) and the short deuteron T_1 value leads to an additional contribution to measured $R_2^{\text{eff}}(\upsilon_{\text{CPMG}})$ rates from scalar relaxation of the second kind[58] that is independent of chemical exchange and varies with υ_{CPMG}. In principle, this unwanted contribution can be suppressed by ^{2}H decoupling during the CPMG periods. Unfortunately, however, we have observed that the application of refocusing pulses during the CPMG intervals interferes with the decoupling process leading to a modulation of the intensity of cross-peaks as a function of υ_{CPMG} that again is unrelated to exchange. Therefore, a different strategy has been developed to ensure that dipolar cross-correlations do not compromise measurement of exchange parameters.

In the Absence of Exchange $R_2^{\text{eff}}(\upsilon_{\text{CPMG}})$ Is Independent of the CPMG Pulse Repetition Rate. With the potential problems described above we have carefully considered the evolution of ^{15}N magnetization in an NH_2 spin system during the interval extending from *a* to *e* in the pulse scheme of Figure 1. A necessary condition for the accurate extraction of exchange parameters from a relaxation dispersion profile is that the only dependence of R_2^{eff} on the CPMG pulse repetition rate derives from the exchange process itself. It is important, therefore, to demonstrate that in the absence of exchange evolution of magnetization is independent of pulse spacing in the constant-time CPMG intervals in the sequence.

Assuming an isolated NH_2 spin system, with the ^{15}N spin on resonance, the evolution of $2N_+H_Z$ ($N_+ = N_X + iN_Y$) between two consecutive ^{15}N 180° pulses in the CPMG trains can be obtained from[59]

$$\frac{\mathrm{d}}{\mathrm{d}t}\begin{pmatrix} N_+ \\ 2N_+H_{Z,1} \\ 2N_+H_{Z,2} \\ 4N_+H_{Z,1}H_{Z,2} \end{pmatrix} = -\begin{pmatrix} \Gamma_1 & i\pi\mathrm{J} & i\pi\mathrm{J} & \Gamma_2 \\ i\pi\mathrm{J} & \Gamma_1+\Gamma_{H1,H2} & \Gamma_2-\Gamma_{H1,H2} & i\pi\mathrm{J} \\ i\pi\mathrm{J} & \Gamma_2-\Gamma_{H1,H2} & \Gamma_1+\Gamma_{H1,H2} & i\pi\mathrm{J} \\ \Gamma_2 & i\pi\mathrm{J} & i\pi\mathrm{J} & \Gamma_1 \end{pmatrix}\begin{pmatrix} N_+ \\ 2N_+H_{Z,1} \\ 2N_+H_{Z,2} \\ 4N_+H_{Z,1}H_{Z,2} \end{pmatrix} \quad (2)$$

In eq 2 the one-bond ^{15}N−^{1}H scalar coupling, J, and the spectral densities of the ^{15}N−^{1}H dipolar interactions are assumed to be the same for the two ^{15}N−^{1}H spin pairs. Only terms proportional to spectral density functions evaluated at zero frequency have been included in the expressions for the elements of the Redfield matrix (macromolecular limit). The values of Γ_1, Γ_2, and $\Gamma_{H1,H2}$ are given by

$$\Gamma_1 = 2\left(\frac{\gamma_N\gamma_H\hbar}{r_{NH}^3}\right)^2 J(0) + \Gamma_{\text{CSA}} \quad (3)$$

$$\Gamma_2 = 2\left(\frac{\gamma_N\gamma_H\hbar}{r_{NH}^3}\right)^2 K(0) \quad (4)$$

$$\Gamma_{H1,H2} = 0.5\left(\frac{\gamma_H^2\hbar}{r_{H1,H2}^3}\right)^2 J(0) \quad (5)$$

where $J(0)$ and $K(0)$ are auto- and cross-correlation spectral densities due to dipolar interactions involving spins of the NH_2 system evaluated at zero frequency, γ_i is the gyromagnetic ratio of spin i, r_{ij} is the distance between spins i and j, and Γ_{CSA} contains contributions to auto-relaxation from ^{15}N CSA. Thus, Γ_1 and Γ_2 contain contributions from auto- and cross-correlated relaxation, respectively, while $\Gamma_{H1,H2}$ derives from auto-relaxation. Cross-correlation effects arising from CSA−dipolar interactions have not been included in eq 2 but are considered in the simulations described below. For the case of spins attached to a molecule undergoing isotropic motion,

$$J(0) = \frac{1}{5}\tau_c, \quad K(0) = \frac{1}{5}P_2(\cos\theta_{H1NH2})\tau_c \quad (6)$$

where τ_c is the overall tumbling time and P_2 is a second-order Legendre polynomial with θ_{H1NH2} the angle between vectors N−H_1 and N−H_2.

Rather than immediately evaluating how magnetization evolves for different CPMG pulse spacings, we first prefer to consider a number of limiting cases. In the limit that each of the CPMG intervals in the sequence is replaced by free precession periods, $\upsilon_{\text{CPMG}} \rightarrow 0$, the relaxation of each multiplet

(54) Vold, R. L.; Vold, R. R. *Prog. Nucl. Magn. Reson. Spectrosc.* **1978**, *12*, 79−133.
(55) Palmer, A. G.; Wright, P. E.; Rance, M. *Chem. Phys. Lett.* **1991**, *185*, 41−46.
(56) Palmer, A. G.; Skelton, N. J.; Chazin, W. J.; Wright, P. E.; Rance, M. *Mol. Phys.* **1992**, *75*, 699−711.
(57) Kay, L. E.; Nicholson, L. K.; Delaglio, F.; Bax, A.; Torchia, D. A. *J. Magn. Reson.* **1992**, *97*, 359−375.
(58) Abragam, A. *Principles of Nuclear Magnetism*; Clarendon Press: Oxford, 1961.
(59) Kay, L. E.; Bull, T. E. *J. Magn. Reson.* **1992**, *99*, 615−622.

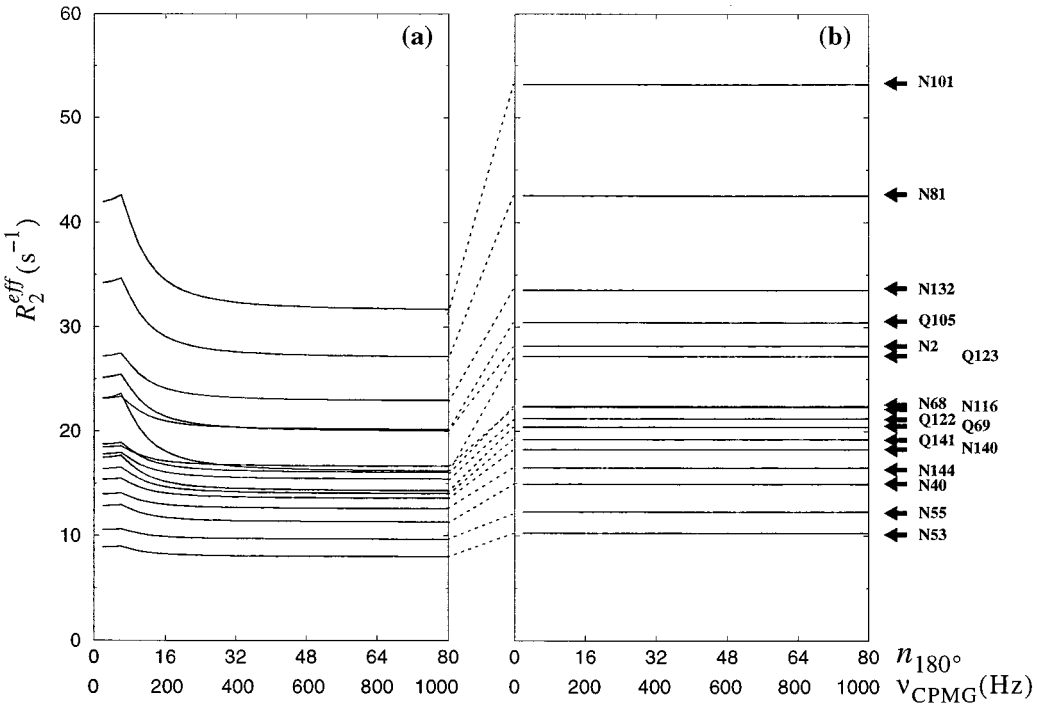

Figure 2. Effective transverse relaxation rates, R_2^{eff}, calculated for the $^{15}N^{\delta 2}$ (Asn) and $^{15}N^{\epsilon 2}$ (Gln) spins of T4 lysozyme as a function of the total number of 180° pulses, $n(180°)$, applied during the two constant-time CPMG periods of total duration T. In (a) a standard CPMG train is employed (i.e., the interval extending from b to d in the sequence of Figure 1 is omitted), and the starting magnetization is N_Y. In (b) the scheme of Figure 1 is employed starting from $2N_YH_Z$ at point a. Details of the simulations are given in the text.

component proceeds independently and eq 2 can be condensed to:

$$\frac{\mathrm{d}}{\mathrm{d}t}\begin{pmatrix}2N_+H_Z\\ N_+ + 4N_+H_{Z,1}H_{Z,2}\end{pmatrix} = -\begin{pmatrix}\Gamma_1+\Gamma_2 & 2i\pi\mathrm{J}\\ 2i\pi\mathrm{J} & \Gamma_1+\Gamma_2\end{pmatrix}\begin{pmatrix}2N_+H_Z\\ N_+ + 4N_+H_{Z,1}H_{Z,2}\end{pmatrix} \quad (7)$$

Note that $2N_+H_Z$ and $N_+ + 4N_+H_{Z,1}H_{Z,2}$ relax with the same rates. Although J-coupling will interchange both components, the relaxation of each will be unaffected.

A second limit of interest is where refocusing pulses are applied rapidly compared to 1/(2J) during the CPMG periods, $\upsilon_{\text{CPMG}} \rightarrow \infty$. In this case scalar coupling evolution is suppressed, while the relaxation of each of the operators, $2N_+H_Z$ and $N_+ + 4N_+H_{Z,1}H_{Z,2}$, remains unchanged ($\Gamma_1 + \Gamma_2$). Thus, in the two limiting cases considered, $\upsilon_{\text{CPMG}} \rightarrow 0$ and $\upsilon_{\text{CPMG}} \rightarrow \infty$, the effective relaxation rate of $2N_+H_Z$ is the same, $\Gamma_1+\Gamma_2$. In fact, it can be easily shown (see below) that the effective relaxation rate of $2N_+H_Z$ remains constant in the absence of chemical exchange throughout the entire range of υ_{CPMG}.

The discussion to this point has focused on an isolated NH_2 spin system, clearly an oversimplification for biomolecules such as proteins. To good accuracy the effects of external protons can be estimated by including contributions to the auto-relaxation rates of the operators listed in eq 2. In this approximation, the auto-relaxation rates (i.e., diagonal elements in eq 2) of $2N_+H_{Z,1}$, $2N_+H_{Z,2}$ and $4N_+H_{Z,1}H_{Z,2}$ are increased by $1/T_{1,s}$, $1/T_{1,s}$ and $2/T_{1,s}$, respectively, where $T_{1,s}$ is the contribution to the selective T_1 of each of the protons (assumed equal) of the NH_2 group from spin flip-flops involving external protons. In principle, contributions to the decay of $2N_+H_{Z,1}$, $2N_+H_{Z,2}$ and $4N_+H_{Z,1}H_{Z,2}$ from exchange with water can also be accounted for by the $T_{1,s}$ terms.[60,61] In the case of external contributions to relaxation, and in the limit that $\upsilon_{\text{CPMG}} \rightarrow 0$, evolution of the spin system during the periods extending from a to b and from d to e is described by a more complex system of equations (see eq 2), via eq 8,

$$\frac{d}{dt}\begin{pmatrix}2N_+H_Z\\ N_+ + 4N_+H_{Z,1}H_{Z,2}\\ N_+ - 4N_+H_{Z,1}H_{Z,2}\end{pmatrix} = -\begin{pmatrix}\Gamma_1+\Gamma_2+\frac{1}{T_{1,s}} & 2i\pi\mathrm{J} & 0\\ 2i\pi\mathrm{J} & \Gamma_1+\Gamma_2+\frac{1}{T_{1,s}} & \frac{-1}{T_{1,s}}\\ 0 & \frac{-1}{T_{1,s}} & \Gamma_1-\Gamma_2+\frac{1}{T_{1,s}}\end{pmatrix}\begin{pmatrix}2N_+H_Z\\ N_+ + 4N_+H_{Z,1}H_{Z,2}\\ N_+ - 4N_+H_{Z,1}H_{Z,2}\end{pmatrix} \quad (8)$$

To investigate the behavior of the system as a function of υ_{CPMG} it is important to consider how both $2N_+H_Z$ and $N_+ + 4N_+H_{Z,1}H_{Z,2}$ relax, since for finite pulse repetition rates $2N_+H_Z$ and $N_+ + 4N_+H_{Z,1}H_{Z,2}$ are interchanged via scalar coupling. (In the limit of $\upsilon_{\text{CPMG}} \rightarrow \infty$ the relaxation of the term of interest, $2N_+H_Z$, is given by $\Gamma_1 + \Gamma_2 + 1/T_{1,s}$). In this regard it is important to consider that (i) during the interval extending from b to d $N_+ + 4N_+H_{Z,1}H_{Z,2}$ and $N_+ - 4N_+H_{Z,1}H_{Z,2}$ are converted to $-(N_- + 4N_-H_{Z,1}H_{Z,2})$ and $N_- - 4N_-H_{Z,1}H_{Z,2}$, respectively, and (ii) the relaxation rates of $2N_+H_Z$ and $N_+ + 4N_+H_{Z,1}H_{Z,2}$ are identical to the rates of the corresponding components obtained by interchanging N_+ and N_-. The cross-relaxation between $N_\pm + 4N_\pm H_{Z,1}H_{Z,2}$ and $N_\pm - 4N_\pm H_{Z,1}H_{Z,2}$ is therefore suppressed to first order by the spin−echo period extending from b to d.

(60) Grzesiek, S.; Bax, A. *J. Biomol. NMR* **1993**, *3*, 627−638.

(61) Skrynnikov, N. R.; Ernst, R. R. *J. Magn. Reson.* **1999**, *137*, 276−280.

The effective relaxation rate of $N_{\pm}+4N_{\pm}H_{Z,1}H_{Z,2}$ over the interval extending from *a* to *e* is thus given by $\Gamma_1+\Gamma_2+1/T_{1,s}$, to good approximation, as long as the CPMG intervals of length $T/2$ are much smaller than $T_{1,s}$. For proteins with correlation times on the order of 10 ns, minimum values of $T_{1,s}$ are on the order of 100 ms, while $T/2 = 20$ ms in present applications. Thus, the effective relaxation rates of $2N_+H_Z$ and $N_+ + 4N_+H_{Z,1}H_{Z,2}$ are the same, and the application of pulses during the CPMG periods will have very little influence (see below) on the monitored relaxation rate when chemical exchange is absent. The utility of the spin−echo interval described above is reminiscent of the role of selective inversion pulses applied during the mixing periods of NOESY experiments to reverse cross-relaxation magnetization transfer.[62] It is noteworthy that Loria, Rance, and Palmer have used a similar approach in the case of AX spin systems to ensure that the effective relaxation of the magnetization of interest is independent of pulse spacing in the CPMG trains.[19]

To rigorously establish the method we have simulated the effective relaxation rate of $2N_YH_Z$ as a function of the number of ^{15}N 180° pulses in the CPMG trains of the pulse sequence of Figure 1 for the $^{15}N^{\delta 2}$ (Asn) and $^{15}N^{\epsilon 2}$ (Gln) spins of T4 lysozyme. These simulations, Figure 2, include an extended relaxation analysis, with contributions from external protons evaluated in a number of different ways (see Materials and Methods for details). The calculations assume an isotropic tumbling model with a rotational correlation time of 10.8 ns,[44] 800 MHz ^{1}H frequency and a CPMG duration, *T*, of 40 ms. All spectral densities including those evaluated at nonzero frequencies, have been included. In panel (a) a hypothetical experiment is considered where the period extending from *b* to *d* in Figure 1 is eliminated and the starting magnetization is N_Y, while in panel (b) the experiment of Figure 1 with the initial spin state $2N_YH_Z$ is simulated. It is clear that for a number of residues in lysozyme the effective transverse relaxation rate, R_2^{eff}, varies considerably with pulse spacing if a standard CPMG period is employed and the initial magnetization is N_Y (panel a). This is particularly the case for residues with substantial $1/T_{1,s}$ rates ($\sim 10\ s^{-1}$) and can be explained by considering eq 8 along the lines of the above discussion.

In contrast, when the starting condition is $2N_YH_Z$ and when the echo period between *b* and *d* in the sequence of Figure 1 is employed R_2^{eff} changes by less than 0.2% as a function of the number of pulses, $n(180°)$, for $T = 40$ ms; the dispersion profile thus would allow an accurate quantification of exchange processes (panel b).

Finally, because of the geometry of the NH_2 group (the H1−N−H2 bond angle is close to 120°) cross-correlation rates are reasonably small, with Γ_2 values on the order of 1 s^{-1} for a protein tumbling with a correlation time of 10 ns. Simulations similar to those described above have also been performed for $^{13}CH_2$ groups, where the geometry is such that cross-correlations are much more significant, showing that the extraction of accurate exchange parameters is not affected by dipole−dipole cross-correlation. Thus the methodology presented in this paper is also applicable to the study of exchange using dispersion profiles of $^{13}CH_2$ moieties, although the rapid decay of ^{13}C magnetization in methylene groups will likely limit applications to small proteins. In general, in cases where sensitivity is critical the value of *T* can be reduced, although this will limit the range of υ_{CPMG} to larger values.

(62) Vincent, S. J.; Zwahlen, C.; Bodenhausen, G. *J. Biomol. NMR* **1996**, *7*, 169−172.

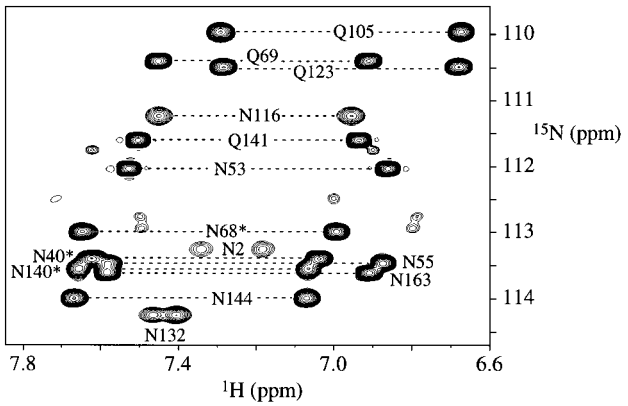

Figure 3. 800 MHz 2D ^{1}H−^{15}N NH_2 correlation map of L99A (1 mM protein, 50 mM sodium phosphate, 25 mM sodium chloride, pH 5.5, 25 °C) recorded using the scheme of Figure 1 with the CPMG periods omitted. Assignments for correlations indicated with * are tentative.

Dispersion Profiles Can Be Interpreted Using Expressions for a Single Spin Undergoing Chemical Exchange. The theory and simulations described above demonstrate that using the scheme of Figure 1, and in the absence of exchange, flat dispersion profiles are obtained for NH_2 spin systems. This is a necessary condition for the extraction of accurate exchange parameters in cases where exchange exists but it is not sufficient. We show below that the dispersion profile for an NH_2 system exchanging between two sites can be analyzed using well-known results derived for a single isolated exchanging spin.[37,38]

The evolution of magnetization exchanging between two sites, *a* and *b*, during the intervals between CPMG pulses, can be described according to

$$\frac{\mathrm{d}}{\mathrm{d}t}\begin{pmatrix} 2N_+^a\,H_Z^a \\ N_+^a + 4N_+^a\,H_{Z,1}^a H_{Z,2}^a \\ 2N_+^b\,H_Z^b \\ N_+^b + 4N_+^b\,H_{Z,1}^b H_{Z,2}^b \end{pmatrix} = -(i\tilde{Z} + i\tilde{J} + \tilde{\Gamma} + \tilde{X})\begin{pmatrix} 2N_+^a\,H_Z^a \\ N_+^a + 4N_+^a\,H_{Z,1}^a H_{Z,2}^a \\ 2N_+^b\,H_Z^b \\ N_+^b + 4N_+^b\,H_{Z,1}^b H_{Z,2}^b \end{pmatrix} \quad (9)$$

where matrixes $\tilde{Z}$, $\tilde{J}$, $\tilde{\Gamma}$, and $\tilde{X}$ contain contributions from chemical shift, scalar coupling, relaxation, and chemical exchange, respectively. Starting from eq 7 it is straightforward to show that

$$i\tilde{Z} + \tilde{\Gamma} + \tilde{X} = \begin{pmatrix} \Gamma_1+\Gamma_2+k_{a\to b}+i\omega_N^a & 0 & -k_{b\to a} & 0 \\ 0 & \Gamma_1+\Gamma_2+k_{a\to b}+i\omega_N^a & 0 & -k_{b\to a} \\ -k_{a\to b} & 0 & \Gamma_1+\Gamma_2+k_{b\to a}+i\omega_N^b & 0 \\ 0 & -k_{a\to b} & 0 & \Gamma_1+\Gamma_2+k_{b\to a}+i\omega_N^b \end{pmatrix} \quad (10)$$

and

$$i\tilde{J} = \begin{pmatrix} 0 & 2i\pi J & 0 & 0 \\ 2i\pi J & 0 & 0 & 0 \\ 0 & 0 & 0 & 2i\pi J \\ 0 & 0 & 2i\pi J & 0 \end{pmatrix} \quad (11)$$

where $k_{a\to b}$ is the rate constant for exchange from site *a* to *b*, ω_N^a is the resonance frequency of the ^{15}N spin in site *a*, spins in sites *a* and *b* are assumed to relax with the same rates,

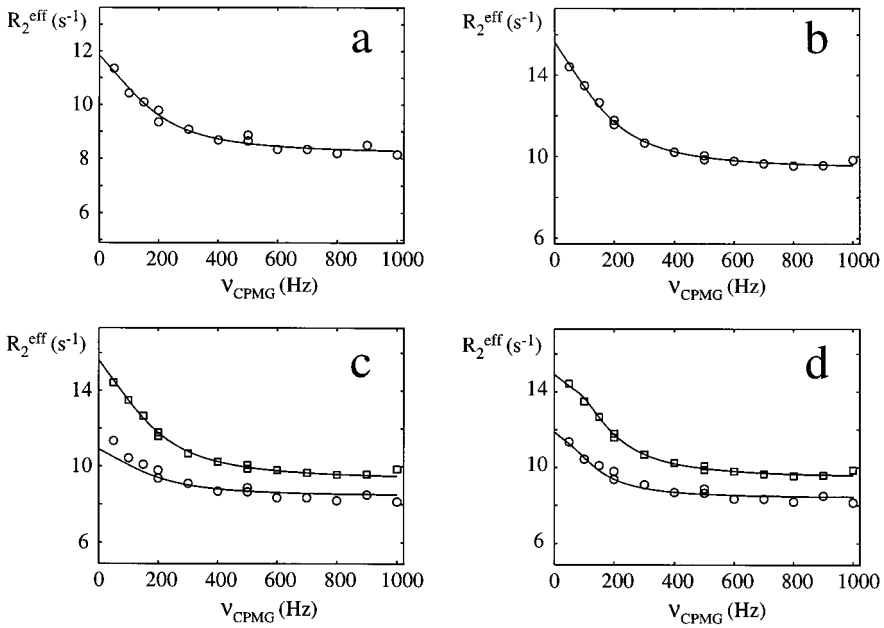

Figure 4. Relaxation dispersion profiles for Gln 105 measured at 500 (a) and 800 (b) MHz and fit with a two-site fast exchange model[23,64] (solid lines). Values of $\tau_{ex} = 0.89$ ms (500 MHz) and 0.85 ms (800 MHz) are obtained. A simultaneous fit of the data at the two fields establishes that the fast exchange assumption is incorrect (c). An excellent simultaneous fit ($\tau_{ex} = 1.52$ ms) is obtained using the general two-site exchange equation[37,38] (d) [see eqs 3−7 of Millet et al.[18]].

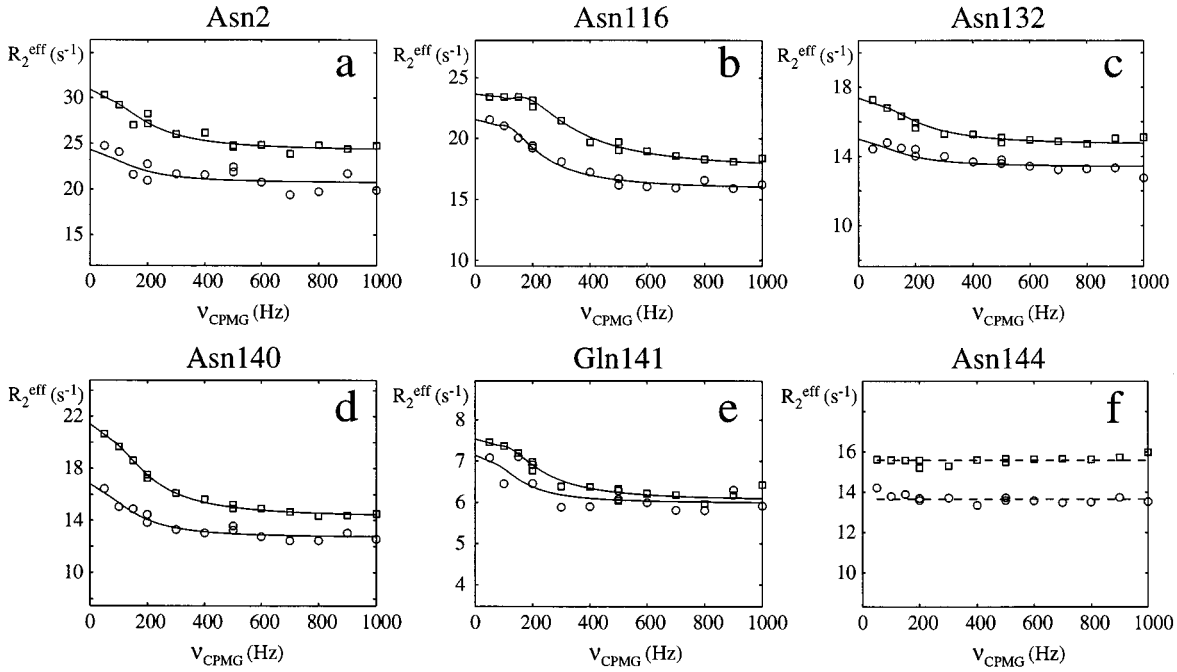

Figure 5. Relaxation dispersion profiles for some of the Asn and Gln residues showing significant R_{ex}, a−e. The solid lines correspond to the best-fit profiles generated from a simultaneous fit of data recorded at 500 and 800 MHz using the general two-site exchange equation. The details of the fits are given in Table 1. In panel f the dispersion profile for a residue without exchange, Asn144, is shown for comparison.

magnetization modes are weighted according to the populations p_a and p_b, and for the moment, external spins are not considered (i.e., the NH_2 group is isolated). Noting that matrixes $i\tilde{J}$ and $i\tilde{Z} + \tilde{\Gamma} + \tilde{X}$ commute, it is straightforward to show that evolution from scalar coupling is completely refocused during a $\tau_{CPMG} - 180°-\tau_{CPMG}$ element from the CPMG sequence of Figure 1 (see Appendix). The magnetization at the end of each $\tau_{CPMG} - 180°-\tau_{CPMG}$ interval is determined, therefore, by the matrices $\pm i\tilde{Z} + \tilde{\Gamma} + \tilde{X}$ (see Appendix). Since the matrix $\pm i\tilde{Z} + \tilde{\Gamma} + \tilde{X}$ is comprised of two uncoupled 2×2 blocks, each of which is formally equivalent to the matrix describing evolution of a single isolated spin exchanging between two sites, the expressions described in the literature can be applied to data from an exchanging XH_2 group as well.[37,38,63]

The above discussion applies to the case where (i) external spins are not considered, (ii) the intrinsic relaxation rates of $H_{Z,1}$ and $H_{Z,2}$ are the same, (iii) dipole−CSA cross-correlations are disregarded, and (iv) the relaxation behavior of the system in sites *a* and *b* is identical. The more general situation where none of these assumptions are made has been investigated using numerical simulations (see Materials and Methods). In particular, simulations include spin−flip relaxation contributions from

(63) Davies, D. G.; Perlman, M. E.; London, R. E. *J. Magn. Reson., Ser. B* **1994**, *104*, 266−275.

external proton spins ($\sim$10 s^{-1}) as well as a 2-fold difference in relaxation rates between sites *a* and *b*. It was found that the dispersion profiles generated in this manner are identical to those obtained for a single-spin exchanging between two sites. Thus, the analysis of data obtained from the pulse scheme of Figure 1 can be performed using closed analytical expressions derived for a single-spin system.

Results and Discussion

Figure 3 shows the 800 MHz 2D $^1H-^{15}N$ NH_2 correlation map of the Leu to Ala99 mutant of T4 lysozyme (1 mM in protein, 25 °C) recorded using the scheme of Figure 1 with the CPMG periods omitted. Fourteen of the expected 17 pairs of correlations are observed. Figure 4a and b illustrate the relaxation dispersion profiles for Gln105 obtained at field strengths of 500 and 800 MHz, respectively. It is worth emphasizing that a complete profile, comprising twelve B_1 fields with two repeat points, was obtained in $\sim$18 h of measuring time using the constant-time approach described above. In Figure 4a and b the dispersion profiles are fit independently to the fast exchange equation,[23,64] yielding $\tau_{ex} = 1/k_{ex}$ values of 0.89 and 0.85 ms at 500 and 800 MHz, respectively. Note that excellent fits to the data are obtained when the fast exchange model is used to fit the data at each field independently. It is clear, however, that when data at the two fields are fit simultaneously assuming fast exchange, Figure 4c, the agreement between model and experiment is much poorer. In Figure 4d a simultaneous fit of the data at the two fields is presented using the general two-site equation[37,38] which makes no assumptions regarding the exchange rate. In this case an excellent fit is obtained, with $\tau_{ex} = 1.52$ ms and an estimated $\alpha = d \ln R_{ex}/d \ln B_o$ value[18] of 0.96, corresponding to intermediate exchange ($R_{ex} = R_2^{eff}(\upsilon_{CPMG} = 0) - R_2^{eff}(\upsilon_{CPMG} = \infty)$ and B_o is the static magnetic field strength). The importance of having data at two independent fields, discussed at some length by Palmer and coworkers,[18] is underscored by the present example. In this regard the ability to record dispersion profiles in a rapid manner is critical.

Figure 5 displays relaxation dispersion profiles recorded at 500 and 800 MHz for a number of Asn and Gln residues in L99A for which significant exchange was observed. By means of comparison, Figure 5f shows profiles obtained for Asn 144 for which exchange was not observed. A summary of the parameters extracted using the general two-site equation, is given in Table 1. Exchange lifetimes, τ_{ex}, vary from about 1 to 2.8 ms, differences in ^{15}N chemical shifts between the two sites are on the order of 1−2 ppm (4 ppm for Asn 116), while the fractional population of the minor conformer is approximately 1−2%. It is important to emphasize that individual N−H correlations for each NH_2 group were fit independently and that averages over the pairs of results are reported in Table 1. Identical parameters should be obtained for each correlation, so that the differences reported provide a measure of the experimental error.

The substitution of Ala for Leu at position 99 of T4 lysozyme enlarges a preexisting completely buried cavity[30,31] to about 150 Å^3, facilitating the rapid binding of a number of ligands such as substituted benzenes and xenon.[32] The X-ray structure of L99A shows that there is not a clear path for ligand entry to the interior of the protein,[30] suggesting that access to the cavity binding site is only possible via a concerted process involving motion of backbone and side chain atoms. To define those residues that may play a role in entry we have recently carried out a backbone ^{15}N spin relaxation study of L99A.[44] A large amount of μs−ms time-scale motion was observed in regions proximal to the Leu → Ala substitution, with backbone amide nitrogens from residues on helices A, E, F, G, and I showing significant exchange (>1 s^{-1}). Notably, these helices are all part of the C-domain containing the cavity mutation. In the present study we have extended probes of dynamics to include

Table 1. Relaxation Dispersion Parameters for Side Chain ^{15}N Spins in L99A at 25 °C[a]

residue	$\omega_N^a - \omega_N^b$ (ppm)[b]	τ_{ex} (ms)[c]	P_a (%)[d]	R_2^{eff} ($\nu_{CPMG} \rightarrow \infty$) ($s^{-1}$) $\omega_0/2\pi =$ 500 MHz	R_2^{eff} ($\nu_{CPMG} \rightarrow \infty$) ($s^{-1}$) $\omega_0/2\pi =$ 800 MHz
Asn 2	1.34 [.32]	1.57 [.46]	2.35 [.78]	21.15 [.47]	24.29 [.08]
Gln 105	1.82 [.10]	1.33 [.19]	1.19 [.11]	8.59 [.19]	9.61 [.16]
Asn 116	3.99 [.07]	2.38 [.20]	1.49 [.08]	15.84 [.01]	17.53 [.03]
Asn 132	1.63 [.28]	2.79 [1.61]	0.76 [.20]	13.87 [.48]	15.02 [.35]
Asn 140	1.66 [.07]	1.17 [.05]	1.61 [.01]	12.31 [.37]	14.02 [.24]
Gln 141	2.32 [.04]	1.97 [.20]	0.33 [.01]	6.01 [.03]	6.05 [.01]

[a] Parameters are obtained by fitting R_2^{eff} (νCPMG) data from $^{15}N^{\epsilon 2}-^1H^{\epsilon 21}$ and $^{15}N^{\epsilon 2}-^1H^{\epsilon 22}$ spectral correlations (Gln) or $^{15}N^{\delta 2}-^1H^{\delta 21}$ and $^{15}N^{\delta 2}-^1H^{\delta 22}$ correlations (Asn) using the general equation for two-site exchange. The average values of parameters are reported together with the uncertainty (shown in square brackets) estimated from the difference between the values obtained from the two correlations. Note that each correlation was fitted independently. [b] Chemical shift difference between the ^{15}N resonances in the two conformers. [c] $\tau_{ex} = (k_{a\rightarrow b} + k_{b\rightarrow a})^{-1}$, where $k_{a\rightarrow b}$ and $k_{b\rightarrow a}$ are the rates of conversion between the two conformers. [d] Population of the minor conformer.

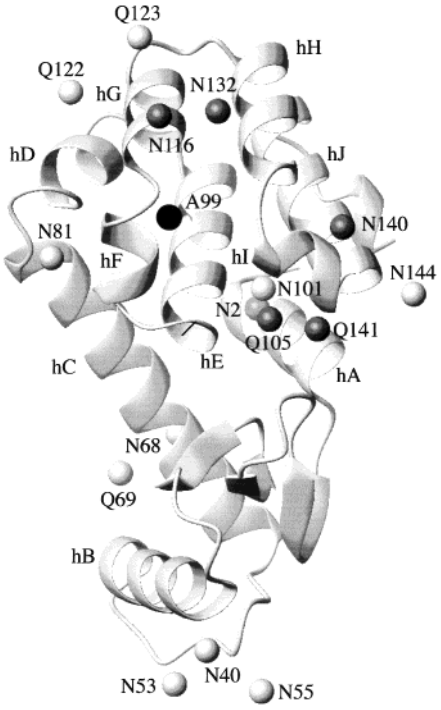

Figure 6. X-ray structure of L99A illustrating the position of the Asn and Gln groups.[69] The position of the Leu→Ala 99 mutation is indicated by the black ball. The dark shaded balls correspond to NH_2 groups with exchange that can be quantified by the relaxation dispersion method described in the text. NH_2 correlations for residues Asn81, Asn101, and Gln122 are unassigned.

(64) Luz, Z.; Meiboom, S. *J. Chem. Phys.* **1963**, *39*, 366−370.
(65) Geen, H.; Freeman, R. *J. Magn. Reson.* **1991**, *93*, 93−141.
(66) Shaka, A. J.; Keeler, J.; Frenkiel, T.; Freeman, R. *J. Magn. Reson.* **1983**, *52*, 335−338.
(67) Schleucher, J.; Sattler, M.; Griesinger, C. *Angew. Chem., Int. Ed. Engl.* **1993**, *32*, 1489−1491.
(68) Marion, D.; Ikura, M.; Tschudin, R.; Bax, A. *J. Magn. Reson.* **1989**, *85*, 393−399.
(69) Eriksson, A. E.; Baase, W. A.; Matthews, B. W. *J. Mol. Biol.* **1993**, *229*, 747−769.

Asn and Gln side chains, illustrated in the L99A structure in Figure 6.

As before, residues in the C-terminus of the protein show slow time-scale dynamics (see Table 1). Gln 105 (E−F loop), Asn 116 (helix G), Asn 140 (helix I), and Gln 141 (helix I) are all in regions where μs−ms dynamics were observed at backbone positions, while Asn 132 is part of helix H where slow motions were not observed previously. Asn 2 immediately precedes helix A, where exchange has been measured at backbone ^{15}N sites. Relaxation dispersion profiles have also been measured for Asn and Gln side chains in T4 lysozyme containing the C54T and C97A mutations but not the cavity L99A substitution. Interestingly, none of the dispersion profiles are consistent with exchange broadening in this protein, strongly suggesting that the exchange observed in L99A is due to the cavity.

In summary, a method has been described for the quantitation of slow exchange processes at side chain Asn and Gln amide positions. The effects of evolution due to the one-bond heteronuclear J-coupling and dipole−dipole cross-correlation between ^{15}N−^{1}H dipoles of NH_2 groups do not prevent accurate extraction of exchange parameters. In addition, the use of constant-time CPMG periods with variable pulse spacing allows measurement of a complete dispersion curve in a short measuring time. The present experiment extends previous studies of slow time-scale motions at backbone positions and is an important addition to the suite of experiments for studying protein dynamics.

Acknowledgment. We thank Dr. Art Palmer (Columbia University, NY) for providing some of the programs used in data analysis and Dr. Ranjith Muhandiram (University of Toronto) for help with the pulse sequence. F.A.A.M. is a postdoctoral fellow with support from the European Molecular Biology Organization (EMBO) and N.R.S. acknowledges a Centennial fellowship from the Medical Research Council of Canada. The research was supported by grants from Natural Sciences and Engineering Research Council of Canada (L.E.K.) and the National Institutes of Health [Grant number GM57766] (F.W.D.). L.E.K. is a foreign investigator of the Howard Hughes Medical Research Institute.

Appendix

Herein we show that if matrixes $i\tilde{J}$ and $i\tilde{Z} + \tilde{\Gamma} + \tilde{X}$ commute then evolution due to scalar coupling is completely refocused during a τ_{CPMG}−180°−τ_{CPMG} element from the CPMG sequence of Figure 1. The solution to eq 9 is given by

$$\begin{pmatrix} 2N^a_+ H^a_Z \\ N^a_+ + 4N^a_+ H^a_{Z,1}H^a_{Z,2} \\ 2N^b_+ H^b_Z \\ N^b_+ + 4N^b_+ H^b_{Z,1}H^b_{Z,2} \end{pmatrix}(\tau_{CPMG}) = \exp\{-(i\tilde{Z} + i\tilde{J} + \tilde{\Gamma} + \tilde{X})\tau_{CPMG}\}\begin{pmatrix} 2N^a_+ H^a_Z \\ N^a_+ + 4N^a_+ H^a_{Z,1}H^a_{Z,2} \\ 2N^b_+ H^b_Z \\ N^b_+ + 4N^b_+ H^b_{Z,1}H^b_{Z,2} \end{pmatrix}(0) \quad \text{(A1)}$$

Subsequent application of a 180° refocusing pulse converts N_+ containing terms to the corresponding N_- operators on the left-hand-side of eq A1. These terms then evolve during the second τ_{CPMG} interval according to

$$\begin{pmatrix} 2N^a_- H^a_Z \\ N^a_- + 4N^a_- H^a_{Z,1}H^a_{Z,2} \\ 2N^b_- H^b_Z \\ N^b_- + 4N^b_- H^b_{Z,1}H^b_{Z,2} \end{pmatrix}(2\tau_{CPMG}) = \exp\{-(-i\tilde{Z} - i\tilde{J} + \tilde{\Gamma} + \tilde{X})\tau_{CPMG}\}\begin{pmatrix} 2N^a_- H^a_Z \\ N^a_- + 4N^a_- H^a_{Z,1}H^a_{Z,2} \\ 2N^b_- H^b_Z \\ N^b_- + 4N^b_- H^b_{Z,1}H^b_{Z,2} \end{pmatrix}(\tau_{CPMG}) \quad \text{(A2)}$$

Substitution of eq A1 into eq A2 gives, in view of the fact that $\tilde{J}$ commutes with $\pm i\tilde{Z} + \tilde{\Gamma} + \tilde{X}$

$$\begin{pmatrix} 2N^a_- H^a_Z \\ N^a_- + 4N^a_- H^a_{Z,1}H^a_{Z,2} \\ 2N^b_- H^b_Z \\ N^b_- + 4N^b_- H^b_{Z,1}H^b_{Z,2} \end{pmatrix}(2\tau_{CPMG}) = \tilde{O}\begin{pmatrix} 2N^a_+ H^a_Z \\ N^a_+ + 4N^a_+ H^a_{Z,1}H^a_{Z,2} \\ 2N^b_+ H^b_Z \\ N^b_+ + 4N^b_+ H^b_{Z,1}H^b_{Z,2} \end{pmatrix}(0) \quad \text{(A3)}$$

where

$$\tilde{O} = \exp\{-(-i\tilde{Z} + \tilde{\Gamma} + X)\}\exp\{-(i\tilde{Z} + \tilde{\Gamma} + \tilde{X})\} \quad \text{(A4)}$$

and the magnetization at $t = 2\tau_{CPMG}$ is independent of J.

JA003447G